**Supporting Information for**

# Highly Productive Electrosynthesis of Ammonia by Admolecule-Targeting Single Ag Sites

*Ying Chen[†], Ruijie Guo[†], Xianyun Peng[†], Xiaoqian Wang[†], Xijun Liu[*], Junqiang Ren, Jia He, Longchao Zhuo, Jiaqiang Sun, Yifan Liu, Yuen Wu[*] and Jun Luo[*]*

[§] Center for Electron Microscopy and Tianjin Key Lab of Advanced Functional Porous Materials, Institute for New Energy Materials & Low-Carbon Technologies, School of Materials Science and Engineering, Tianjin University of Technology, Tianjin 300384, China

[#] School of Chemistry and Materials Science, iChEM, CAS Center for Excellence in Nanoscience, University of Science and Technology of China, Hefei National Laboratory for Physical Sciences at the Microscale, Hefei 230026, China

[$] State Key Laboratory of Advanced Processing and Recycling of Nonferrous Metals, Lanzhou University of Technology, Lanzhou 730050, China

[⊥] School of Materials Science and Engineering, Xi'an University of Technology, Xi'an 710048, China

[&] State Key Laboratory of Coal Conversion, Institute of Coal Chemistry, Chinese Academy of Sciences, Taiyuan 030001, China

¶ College of Physics and Optoelectronic Engineering, Shenzhen University, Shenzhen 518060, China

[†]These authors contributed equally to this work.

* e-mail: xjliu@tjut.edu.cn (X.J.L.); yuenwu@ustc.edu.cn (Y.E.W); jluo@tjut.edu.cn (J.L)


**Figure S1. Massive production of SA-Ag/NC.** By our synthesis method with 0.2 g carbon black, 0.109 g silver nitrate and 2 g urea, one batch of produced SA-Ag/NC has a volume of 4 mL and the mass of 460 mg, which are limited only by the capacity of the porcelain boat used in the pyrolysis. If larger porcelain boats are used, the production yield of SA-Ag/NC can be easily scaled up.

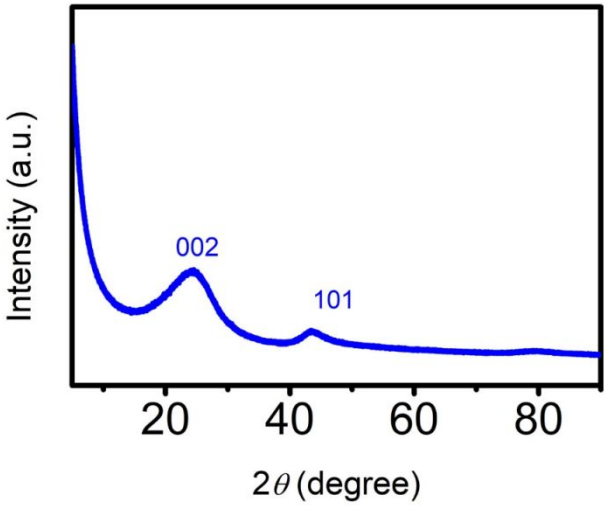


**Figure S2. XRD pattern of the as-synthesized SA-Ag/NC catalyst.** It can be clearly seen that only two characteristic carbon {002} and {101} diffraction humps at approximately 25° and 44° are observed, suggesting the absence of Ag crystals in SA-Ag/NC. This is consistent with the SAED pattern in Figure 2b

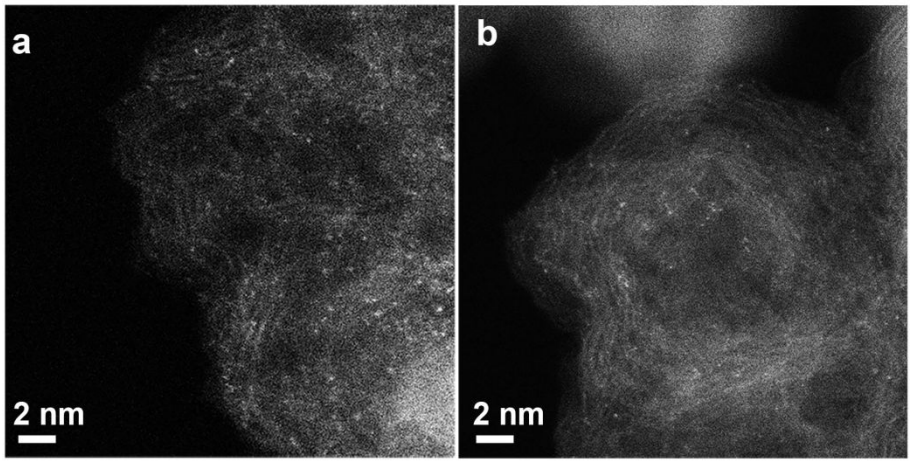


**Figure S3. Additional aberration-corrected HAADF-STEM images of the as-synthesized SA-Ag/NC catalyst.** The bright dots are Ag SAs.

.

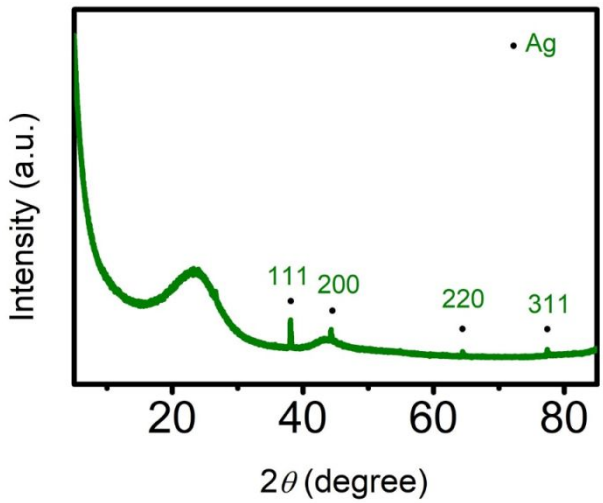


**Figure S4. XRD pattern of the as-synthesized NP-Ag/NC catalyst.** As observed, diffraction peaks attributed to metallic Ag crystals were detected, according to No. 04-0783 of powder diffraction file.

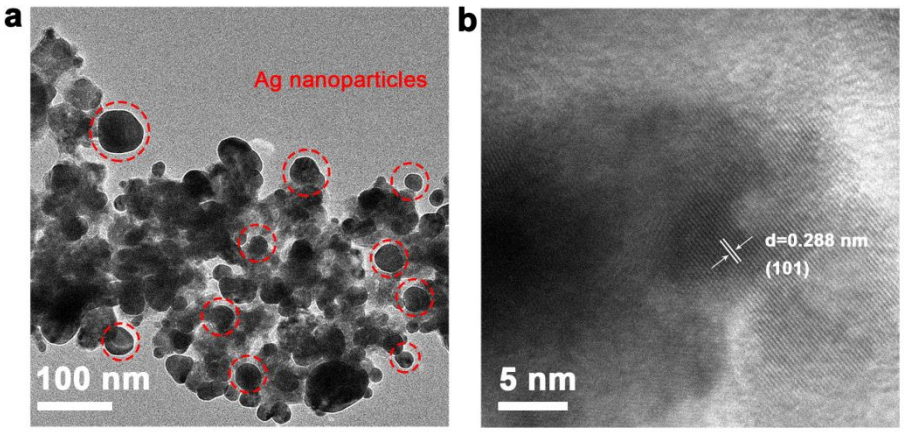


**Figure S5. TEM (a) and HRTEM (b) images of the as-synthesized NP-Ag/NC catalyst.** Clearly, Ag nanoparticles were observed, and some of the nanoparticles in a are highlighted by red circles.

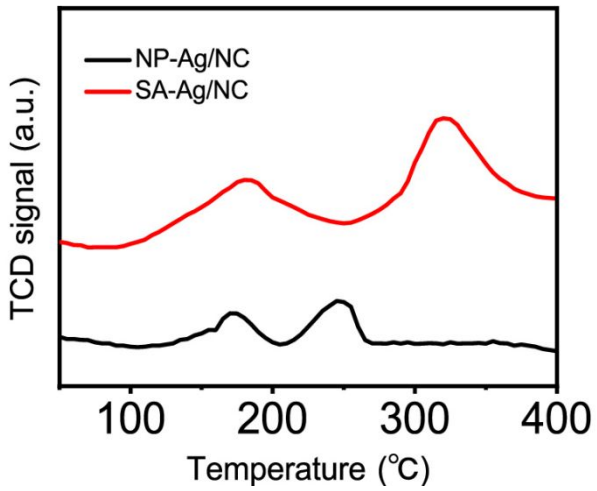


**Figure S6. $N_2$-TPD curves of SA-Ag/NC and NP-Ag/NC.** Earlier work has established the latter peak cane be attributed to the chemisorption of $N_2$ on Ag species[13]. The higher temperature contributes a stronger binding strength of $N_2$ on SA-Ag/NC, thus leading an enhanced NRR activity.

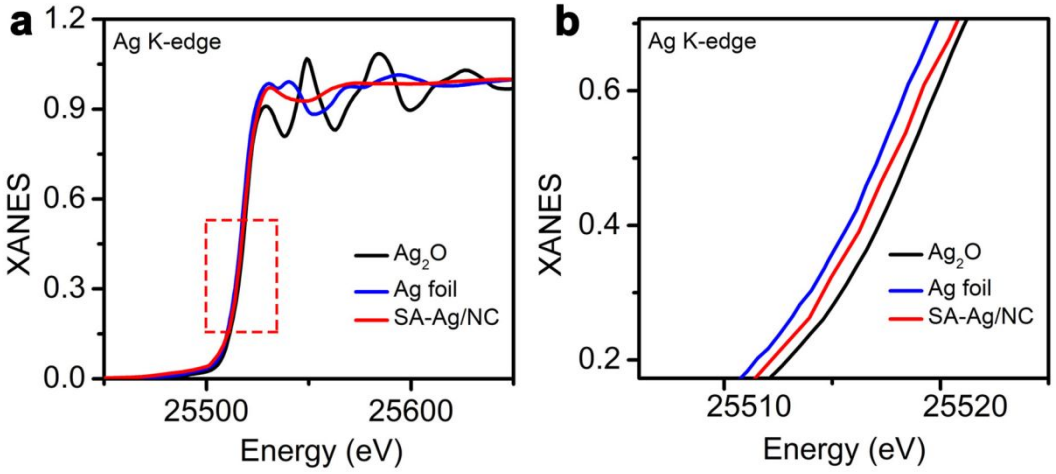


**Figure S7. Ag K-edge XANES spectra (a) and an enlarged image (b).** The enlarged image is from the boxed region in (a). The spectra in (a) are the same ones in Figure 3a.

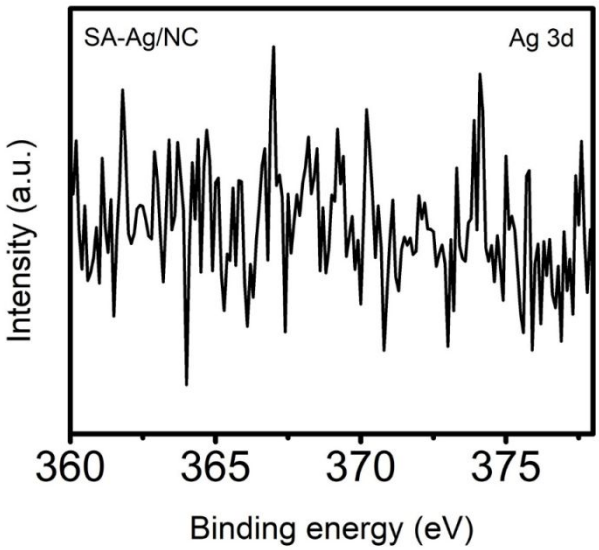


**Figure S8. XPS Ag 3d spectrum of SA-Ag/NC.** Only noise exists in the spectrum.

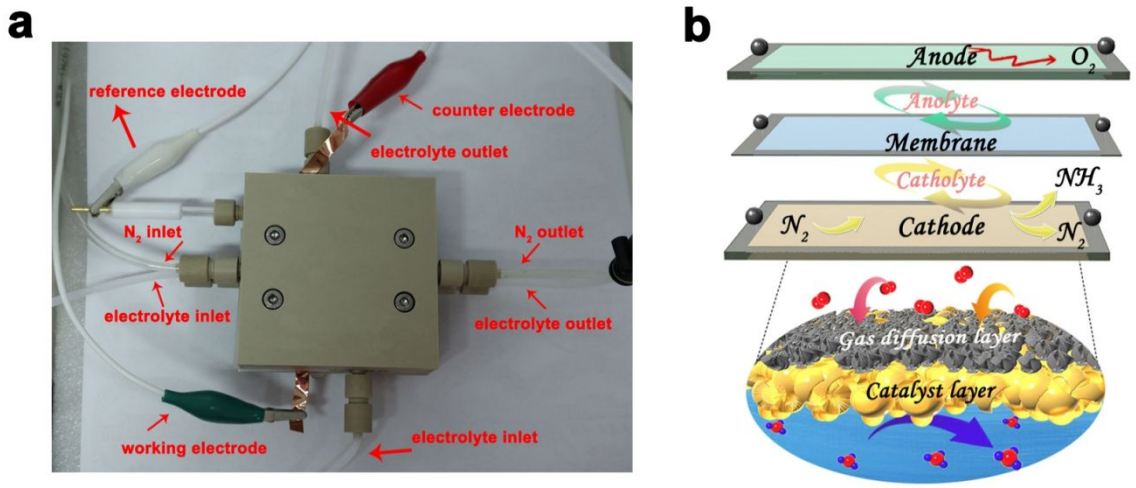


**Figure S9. (a) The optical photograph and (b) the scheme of the electrochemical cell.**

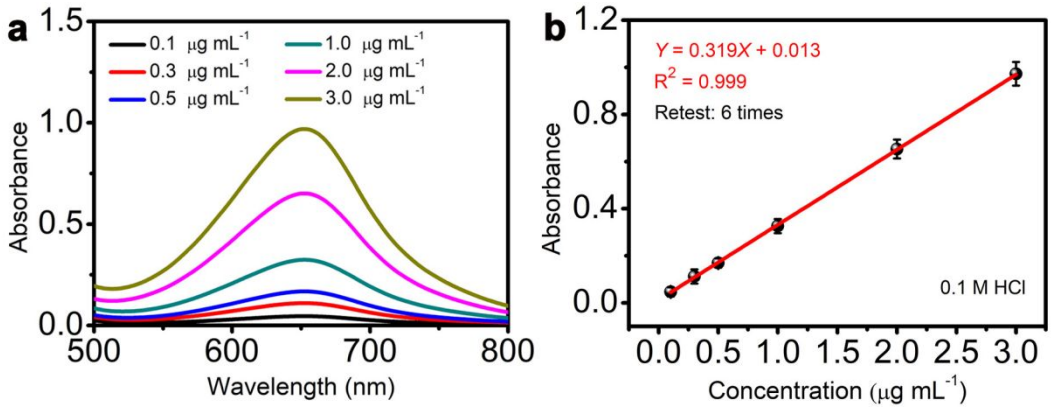


**Figure S10. Calibration line for colorimetric $NH_3$ assay *via* the indophenol blue method.** (a, b) UV-Vis spectra of $NH_4^+$ ion solutions with a series of standard concentrations (a) and the corresponding concentration-absorbance calibration line (b). The data points in (b) were made using the peak absorbance values at 655 nm and their corresponding $NH_4^+$ concentrations in (a). Each error bar of the data points was made by the standard deviation of six measurements. The red line in (b) is the linear fit ($Y = 0.319X + 0.013$) of the data points, and it is the calibration line. By this linear fit equation and the widely used indophenol blue method, the concentration of $NH_3$ produced by an NRR experiment can be determined as follows. Firstly, the catholyte containing the $NH_4^+$ ions produced by the NRR experiment is mixed with indophenol blue. Secondly, the absorbance value of the catholyte is measured at 655 nm. Thirdly, by this absorbance value and the linear fit equation, the $NH_4^+$ concentration value is obtained. For instance, the concentration of $NH_3$ produced by the NRR experiment of SA-Ag/NC in 0.1 M HCl at –0.60 V *vs* RHE for 2 h was measured to be 322.2 μM. That is, $c_{NH3} = 322.2$ μM. Further, the $NH_3$ yield ($y_{NH3}$) can be obtained by $y_{NH3} = c_{NH3} \times V$, where $V$ is the volume of electrolyte (20 mL in this work). More details are given in our previous work.[6]

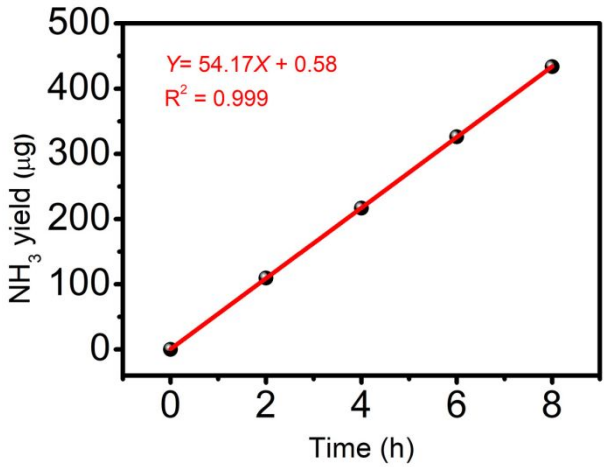


**Figure S11. The curve of $NH_3$ yield *vs* reaction time at –0.60 V *vs* RHE in 0.1 M HCl with SA-Ag/NC, in which the $NH_3$ yield values of the data points were obtained by the indophenol blue method in Figure S8.** The red line is a linear fit, whose slope gives the value of the $NH_3$ yield rate ($R_{NH3}$) to be 54.2 μg $h^{-1}$. When the yield rate is normalized to the mass loading of catalyst (0.2 mg $cm^{-2}$), it becomes 270.9 $\mu g_{NH3}$ $h^{-1}$ $mg_{cat.}^{-1}$ and can be denoted as $r_{NH3}$. More details are given in our previous work[6,15].

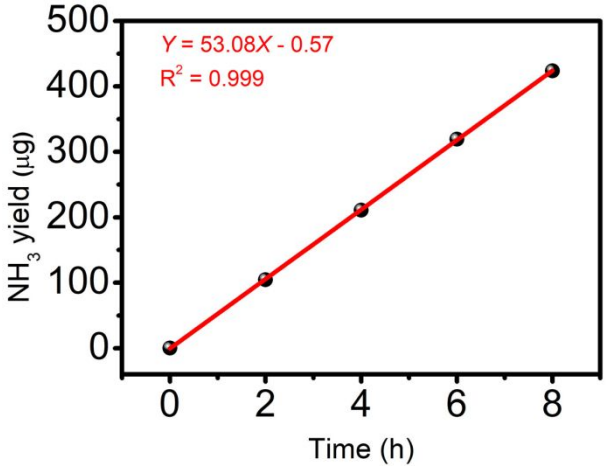


**Figure S12. The curve of $NH_3$ yield *vs* reaction time at –0.60 V *vs* RHE in 0.1 M HCl with SA-Ag/NC, in which the $NH_3$ yield values of the data points were obtained by the ion chromatography.** The red line is a linear fit, whose slope gives the value of the $NH_3$ yield rate ($R_{NH3}$) to be 53.1 μg $h^{-1}$. Then, the mass-normalized yield rate is calculated to be 265.4 $\mu g_{NH3}$ $h^{-1}$ $mg_{cat.}^{-1}$, very close to the corresponding value measured with the indophenol blue method (270.9 $\mu gNH_3$ $h^{-1}$ $mg_{cat.}^{-1}$ in Figure S10).

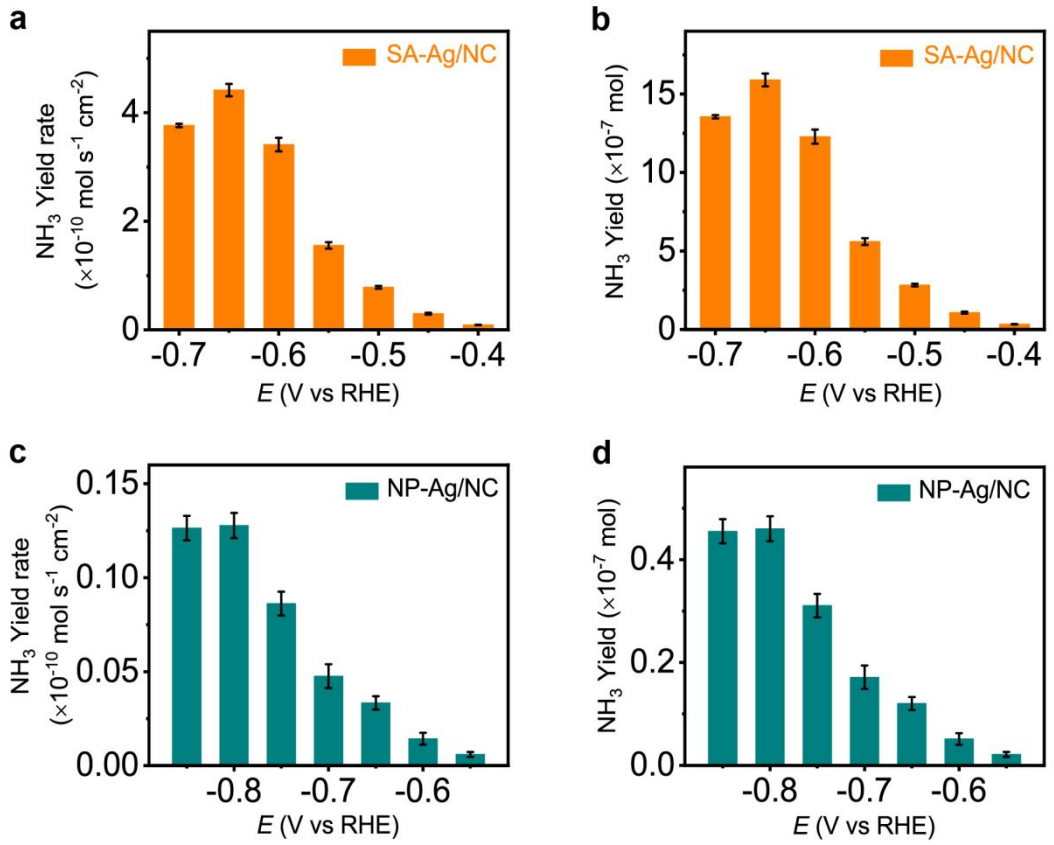


**Figure S13. (a, c) The $NH_3$ yield rates expressed as the moles per unit time per area of the electrode (mol $h^{-1}$ $cm^{-2}$), and (b, d) the actual amount of ammonia produced in one hour over SA-Ag/NC and NP-Ag/NC catalysts, respectively.**

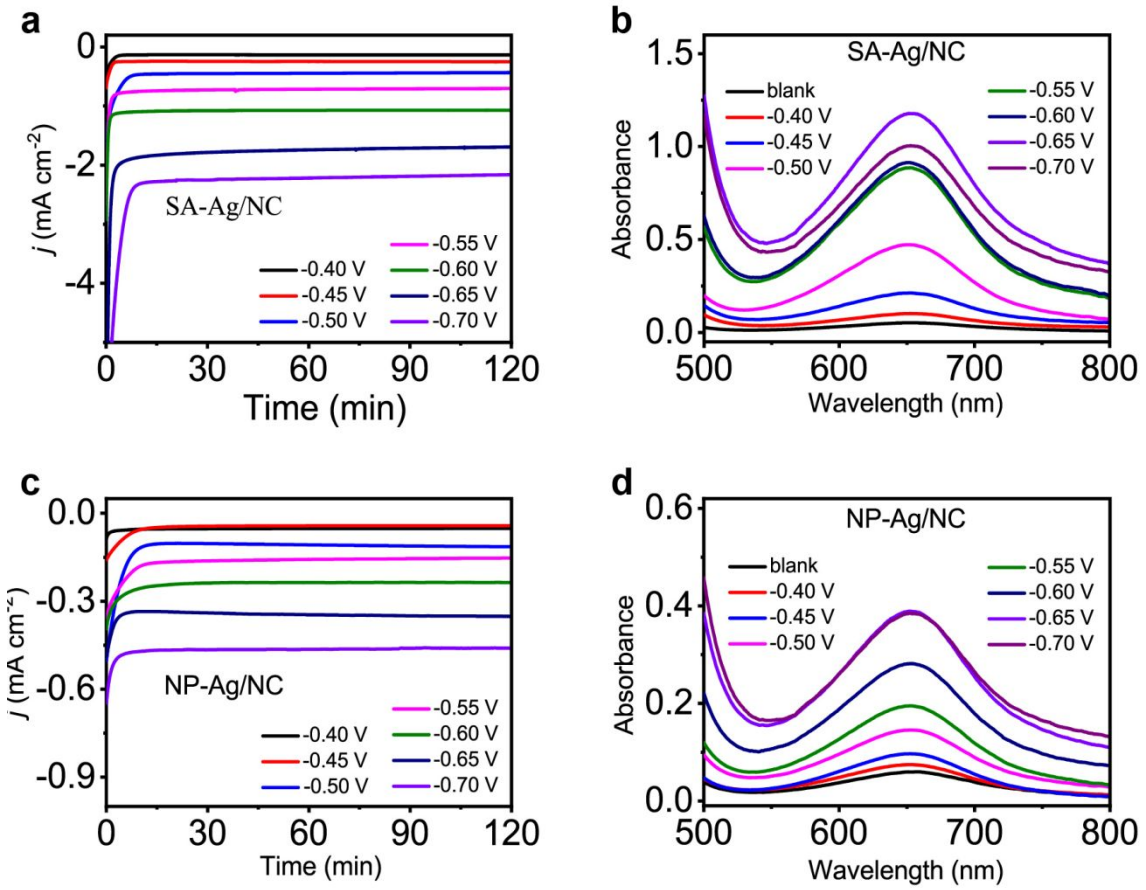


**Figure S14. The *j-t* curves and UV-Vis absorption spectra of SA-Ag/NC (a, b) and NP-Ag/NC (c, d) at the different applied potentials.** To meet the requirement of Lambert-Beer law, the obtained $N_2$-saturated catholytes after 2-h electrolysis at –0.60, –0.65 and –0.70 V *vs* RHE using SA-Ag/NC as the cathode were tested by double dilution method in tubes.

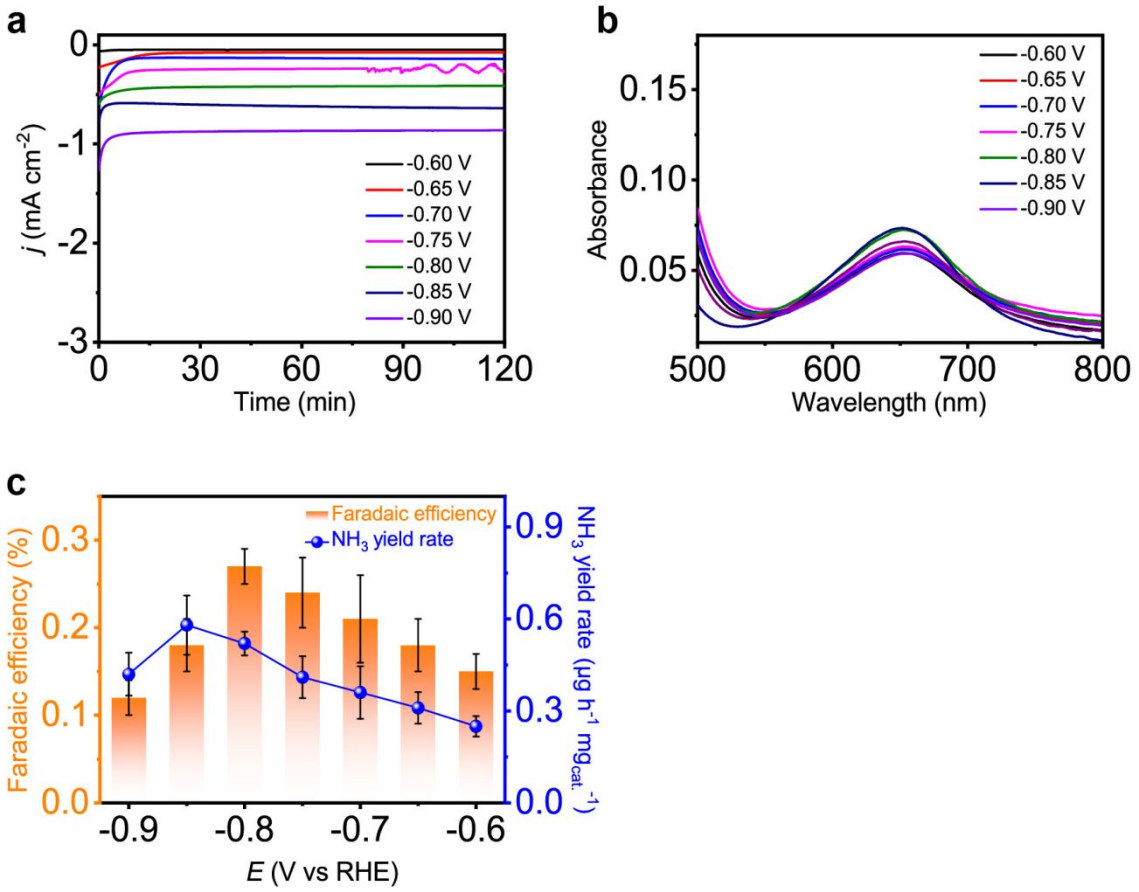


**Figure S15. The NRR performances of NC: (a) The *j-t* curves; (b) UV-Vis absorption spectra; (c) Calculated FEs and yield rates of $NH_3$ over NC.** Compared with SA-Ag/NC and NP-Ag/NC (Figure 4b,c), the maximum $NH_3$ yield rate of NC is negligible, indicating that NC is essentially inactive for NRR.

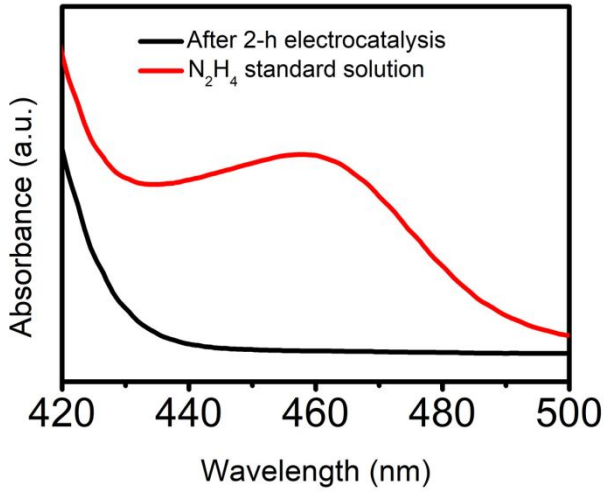


**Figure S16. UV-Vis absorption spectra of an $N_2H_4$ standard solution and a catholyte through a 2-h NRR experiment with SA-Ag/NC at –0.60 V *vs* RHE.** The two solutions had been colored by the Watt and Chrisp method.[10] Typically, a mixture of 0.599 g para-(dimethylamino) benzaldehyde ($C_9H_{11}NO$), 3 mL HCl solution (12 mol/L) and 30 mL ethanol was used as the color reagent for the Watt and Chrisp method. For this UV-vis absorption measurement, 2 mL of the catholyte was mixed with 2 mL of the color reagent. The same volume was used for the $N_2H_4$ standard solution. Comparing the two UV-vis absorption spectra indicates that no $N_2H_4$ signals were detected from the NRR experiment with SA-Ag/NC.

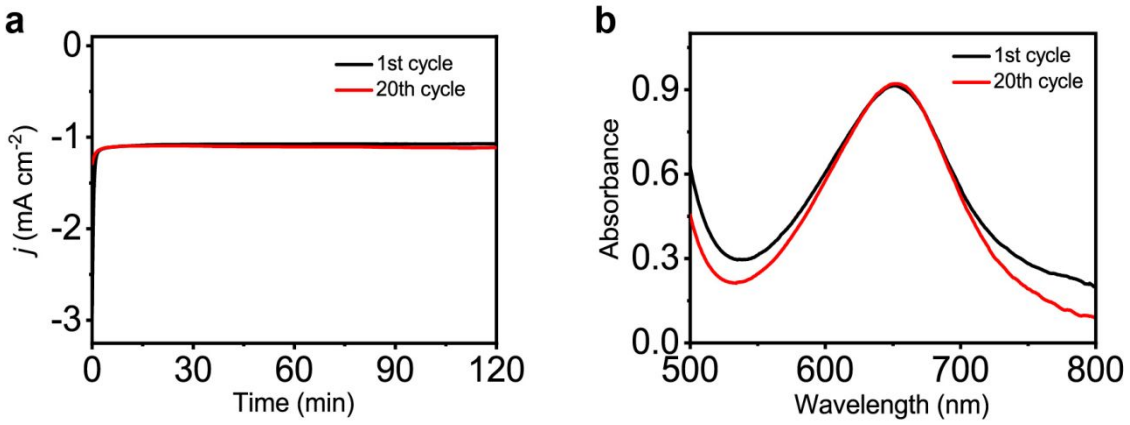


**Figure S17. The *j-t* curves and UV-Vis absorption spectra of SA-Ag/NC at the 1st and 20th cycle tests, respectively.** As seen, the reduction current densities and the corresponding UV-Vis spectra of catholytes still remain stable during the 20 consecutive cycle tests.

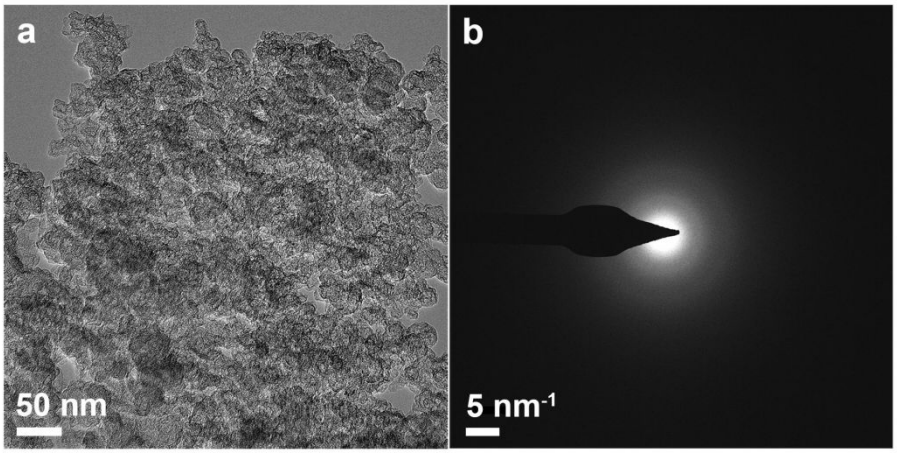


**Figure S18. TEM image and the corresponding SAED pattern of SA-Ag/NC after the 20 consecutive cycle tests.** This image and the pattern reveal that no visible Ag nanoparticles or clusters exist in the tested SA-Ag/NC sample, the same as those results in Figure 2b for as-prepared SA-Ag/NC.

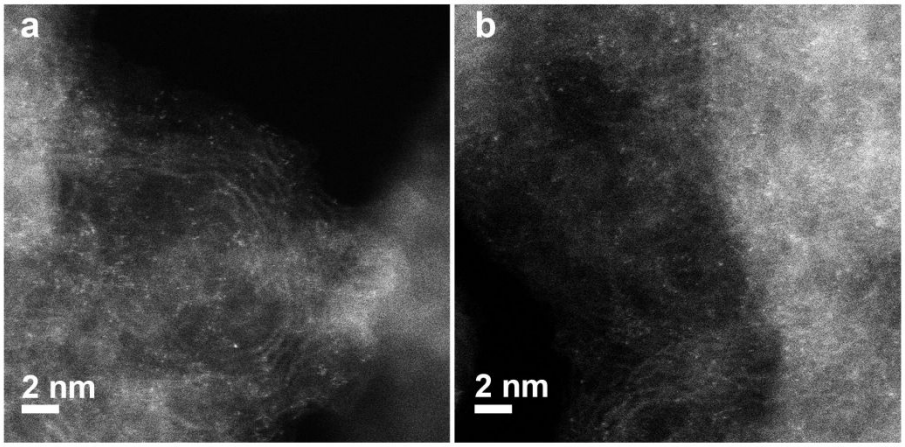


**Figure S19. Aberration-corrected HAADF-STEM images of SA-Ag/NC after the 20 consecutive cycle tests, demonstrating the high stability of the atomically dispersed Ag sites.**

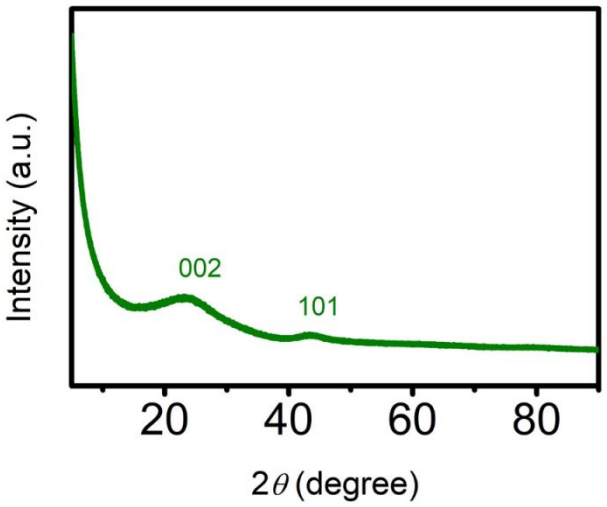


**Figure S20. XRD pattern of SA-Ag/NC after the 20 consecutive cycle tests.** Obviously, no peaks related to Ag nanoparticles or other Ag species exist in this XRD pattern, the same as the XRD result in Figure S2 for as-prepared SA-Ag/NC

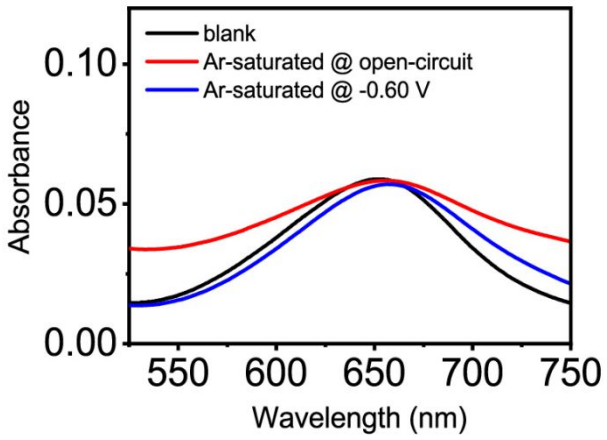


**Figure S21. UV-Vis absorption spectra of Ar-saturated catholytes after 2-h electrolysis at open circuit and –0.60 V *vs* RHE using bare carbon papers as the cathode.** The spectra were obtained by the indophenol blue method.

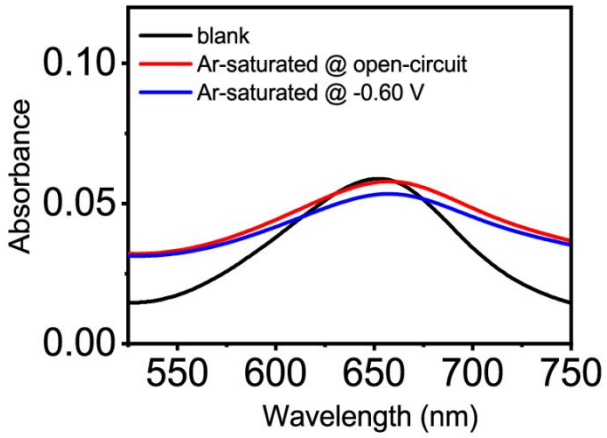


**Figure S22. UV-Vis absorption spectra of Ar-saturated catholytes after 2-h electrolysis at open circuit and –0.60 V *vs* RHE using SA-Ag/NC as the cathode.** The spectra were obtained by the indophenol blue method.

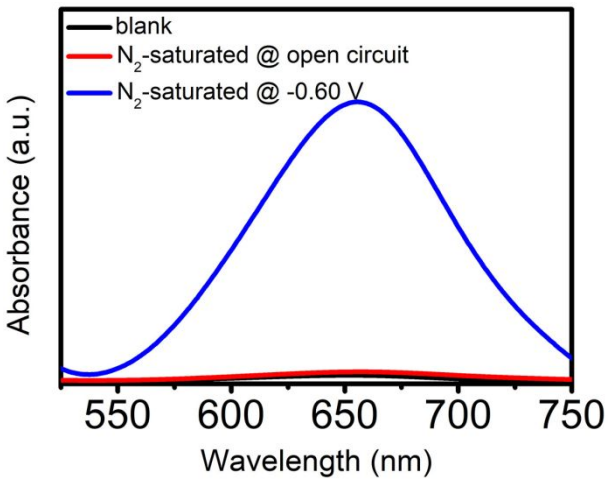


**Figure S23. UV-Vis absorption spectra of $N_2$-saturated catholytes after 2-h electrolysis at open circuit and –0.60 V *vs* RHE using SA-Ag/NC as the cathode.** The spectra were obtained by the indophenol blue method.

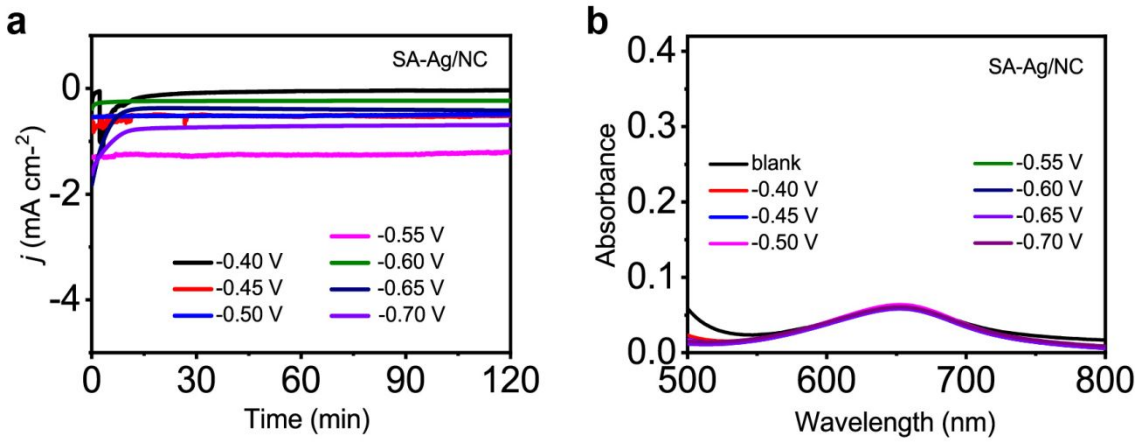


**Figure S24. (a) The *j-t* curves and (b) UV-Vis absorption spectra of SA-Ag/NC under Ar-saturated catholytes for 2 h at the different applied potentials.**

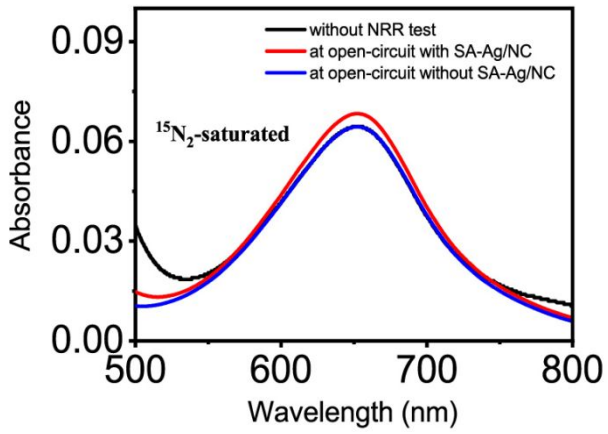


**Figure S25. UV-Vis absorption spectra of $^{15}N_2$-saturated catholytes after 2-h electrolysis under different conditions.**

**Table S1. Performance comparison of non-precious-metal-based, precious-metal-based and metal-free NRR electrocatalysts in aqueous solutions under ambient conditions.**

| Catalyst | Electrolyte | Catalyst Loading (mg cm$^{-2}$) | Onset Potential (V *vs* RHE) | $NH_3$ Yield Rate | | FE (%) | Potential (V *vs* RHE) | Reference |
|---|---|---|---|---|---|---|---|---|
| | | | | μg h$^{-1}$ mg$_{cat.}^{-1}$ | mg h$^{-1}$ mg$_{metal}^{-1}$ | | | |
| **$Mo_2C$ nanorod** | 0.1 M HCl | 0.4 | – | 95.1 | –[a] | 8.1 | –0.30 | *ACS Cent. Sci.* **2019,** *5,* 116 |
| **$Mo_2N$ nanorod** | 0.1 M HCl | – | – | 78.4 | – | 4.5 | –0.30 | *Chem. Commun.* **2018,** *54,* 8474 |
| **$Nb_2O_5$ nanofiber** | 0.1 M HCl | – | – | 43.6 | – | 9.3 | –0.55 | *Nano Energy* **2018,** *52,* 264 |
| **$MoO_3$ nanosheet** | 0.1 M HCl | 1 | – | 29.4 | – | 1.9 | –0.50 | *J. Mater. Chem. A* **2018,** *6,* 12974 |
| **$Cr_2O_3$ nanofiber** | 0.1 M HCl | 0.1 | – | 28.1 | – | 8.6 | –0.75 | *Chem. Commun.* **2018,** *54,* 12848 |
| **$B_4C$** | 0.1 M HCl | 0.1 | – | 26.6 | – | ~16.0 | –0.75 | *Nat. Commun.* **2018,** *9,* 3485 |
| **$Bi_4V_2O_{11}/CeO_2$** | 0.1 M HCl | 2 | – | 23.2 | – | 10.2 | –0.20 | *Angew. Chem. Int. Ed.* **2018,** *57,* 6073 |

| | | | | | | | | |
|---|---|---|---|---|---|---|---|---|
| **$Au/TiO_2$ Au (1.542 wt%)** | 0.1 M HCl | 1 | – | 21.4 | 1.4 (Au) | 8.1 | –0.20 | *Adv. Mater.* **2017,** *29,* 1606550 |
| **NCF-900** | 0.1 M HCl | 4 | – | 15.7 | – | ~1.5 | –0.20 | *J. Mater. Chem. A* **2018,** *6,* 7762 |
| **a-Au/$CeO_x$-RGO Au (1.31 wt%)** | 0.1 M HCl | 200 | – | 8.3 | 0.6 (Au) | 10.1 | –0.20 | *Adv. Mater.* **2017,** *29,* 1700001 |
| **NPC** | 0.1 M HCl | 200 | – | 1.0 | – | 4.2 | –0.20 | *Chem. Commun.* **2019,** *55,* 687 |
| **PCN-NV4** | 0.1 M HCl | 4 | – | 8.1 | – | 11.6 | –0.20 | *Angew. Chem. Int. Ed.* **2018,** *57,* 10246 |
| **FL-BP NSs** | 0.01 M HCl | 0.2 | – | 31.4 | – | 5.1 | –0.70 | *Angew. Chem. Int. Ed.* **2019,** *58,* 2612 |
| **Ru SAs/N-C** | 0.05 M $H_2SO_4$ | 0.255 | – | 120.9 | – | 29.6 | –0.20 | *Adv. Mater.* **2018,** *30,* 1803498 |
| **N-doped porous carbon** | 0.05 M $H_2SO_4$ | 0.4 | –0.38 | 23.8 | – | 1.4 | –0.90 | *ACS Catal.* **2018,** *8,* 1186 |
| **$Au_1/C_3N_4$** | 5 mM $H_2SO_4$ | 0.96 | – | 2.0 | 1.3 (Au) | 11.1 | –0.10 | *Science Bulletin* |

| | | | | | | | | |
|---|---|---|---|---|---|---|---|---|
| | | | | | | | | **2018,** *63,* 1246 |
| **$MoS_2$-rGO** | 0.1 M $LiClO_4$ | 0.1 | – | 24.8 | – | 4.6 | –0.45 | *J. Mater. Chem. A* **2019**, *7,* 2524 |
| **$Mo_2C$/C** | 0.5 M $Li_2SO_4$ | – | – | 34.2 | – | 7.8 | –0.30 | *Adv. Mater.* **2018,** *30,* 1803694 |
| **NCM-Au Au (6.03 wt%)** | 0.1 M HCl | – | – | – | – | 22 | –0.20 | *Angew. Chem. Int. Ed.* **2018,** *57*, 12360 |
| **Bi nanocrystals** | 0.5 M $K_2SO_4$ (pH = 3.5) | – | – | – | 3.4 (Bi) | 66 | –0.60 | *Nat. Catal.* **2019,** *2, 448* |
| **MHCMs** | 0.1 M $Na_2SO_4$ | 0.12 | – | 25.3 | – | 6.8 | –0.90 | *ACS Catal.* **2018,** *8,* 8540 |
| **SA-Mo/NPC** | 0.1 M KOH | 1.0 | – | ~34.0 | – | ~14.6 | –0.30 | *Angew. Chem. Int. Ed.* **2018,** *58*, 2321 |
| **Fe-N/C-CNTs** | 0.1 M KOH | 0.5 | – | 34.8 | – | 9.3 | –0.20 | *ACS Catal.* **2019,** *9,* 336 |
| **Rh NNs** | 0.1 M KOH | 0.32 | – | 23.9 | – | 0.2 | –0.20 | *J. Mater. Chem.A* **2018,** *6,* 3211 |

| | | | | | | | | |
|---|---|---|---|---|---|---|---|---|
| **Ru@$ZrO_2$/NC** | 0.1 M HCl | – | – | – | 3.7 (Ru; –0.21 V *vs* RHE) | ~21 | –0.11 | *Chem* **2019**, *5*, 204 |
| **Au flower** | 0.1 M HCl | 0.6 | – | 25.6 | – | 6.1 | –0.20 | *ChemSusChem* **2018**, *11*, 3480 |
| **Ru nanosheets** | 0.1 M KOH | – | – | 23.9 | – | 0.2 | –0.20 | *J. Mater. Chem. A* **2018**, *6*, 3211 |
| **SA-Fe/NC** | 0.1 M PBS | 1.0 | – | ~62.9 | – | ~18.6 | –0.40 | *Nano Energy* **2019**, 61, 420 |
| **Pd/C** | 0.1 M PBS | – | – | 4.5 | – | 8.2 | 0.10 | *Nat. Commun.* **2018**, *9*, 1975 |
| **$MoS_2$/BCCF** | 0.1 M $Li_2SO_4$ | – | – | 43.4 | – | 9.81 | –0.20 | *Adv. Energy Mater.* **2019**, *9*, 1803935 |
| **Bi nanosheet** | 0.1 M $Na_2SO_4$ | – | – | 13.23 | – | 10.46 | –0.80 | *ACS Catal.***2019**, *9*, 2902 |
| **NPG@ZIF-8** | 0.1 M $Na_2SO_4$ | – | – | – | – | 44 | –0.60 | *Angew. Chem. Int. Ed.* **2019**,10.1002/anie.201909770 |
| **$NbO_2$** | 0.05 M $H_2SO_4$ | 1 | – | 11.6 | – | 32 | –0.60 | *Small Methods* **2019**, *3*,1800386 |
| **$W_2N_3$** | 0.1 M KOH | 0.2 | – | 11.66 | – | 11.67 | –0.20 | *Adv. Mater.* |

| | | | | | | | | |
|---|---|---|---|---|---|---|---|---|
| | | | | | | | | **2019**, *31*, 1902709 |
| **SA-Ag/NC** | 0.1 M HCl | 0.2 | –0.38 | 270.9 (–0.65 V *vs* RHE) | 69.4 (Ag, –0.65 V *vs* RHE) | 21.9 | –0.60 | ***This work*** |

**[a] All of "–" mean that no values were reported for the corresponding parameters in the corresponding references.**

**Table S2. Adsorption structures and the corresponding binding energy of intermediate species, ΔE, in different mechanisms for NRR on SA-Ag/NC surface in eV.** Fe (red), Ag (light blue), N (blue), C (grey) and H (white).

| SA-Fe/NC | | | | | | | | |
|---|---|---|---|---|---|---|---|---|
| Alternating | | | Distal | | | Enzymatic | | |
| species | configurations | ΔE (eV) | species | configurations | ΔE (eV) | species | configurations | ΔE (eV) |
| NN* | 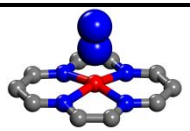 | -0.73 | NN* | 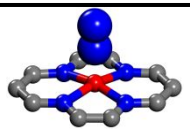 | -0.73 | NN* | 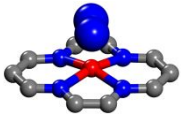 | 0.17 |
| NNH* | 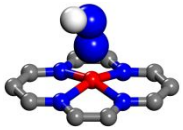 | 1.01 | NNH* | 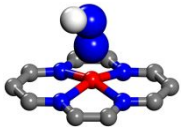 | 1.01 | NNH* | 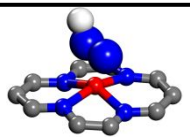 | 1.53 |
| NHNH* | 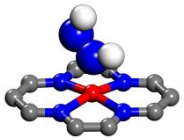 | 0.05 | $NNH_2$* | 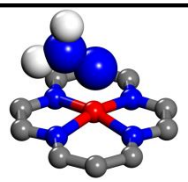 | 0.18 | NHNH* | 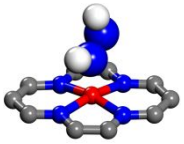 | 0.07 |
| $NHNH_2$* | 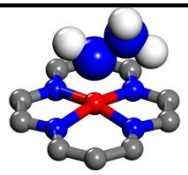 | -0.20 | N* | 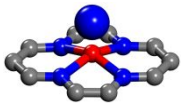 | 2.32 | $NHNH_2$* | 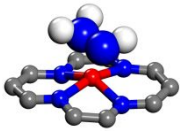 | 0.17 |

| | | | | | | | | |
|---|---|---|---|---|---|---|---|---|
| $NH_2NH_2$* | 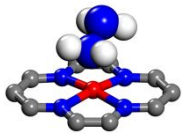 | -1.42 | NH* | 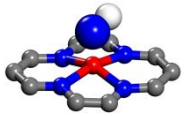 | 1.22 | $NH_2NH_2$* | 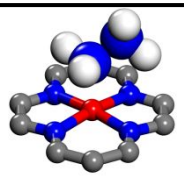 | -1.40 |
| $NH_2$* | 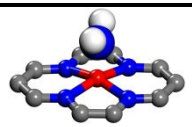 | -0.69 | $NH_2$* | 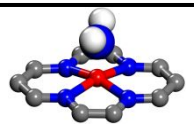 | -0.69 | $NH_2$* | 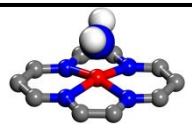 | -0.69 |
| $NH_3$* | 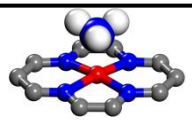 | -2.21 | $NH_3$* | 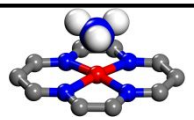 | -2.21 | $NH_3$* | 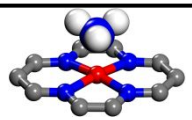 | -2.21 |
| SA-Ag/NC | | | | | | | | |
| Alternating | | | Distal | | | Enzymatic | | |
| species | configurations | ΔE (eV) | species | configurations | ΔE (eV) | species | configurations | ΔE (eV) |
| NN* | 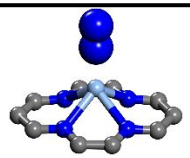 | -0.51 | NN* | 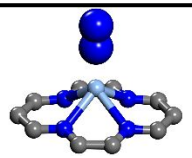 | -0.51 | NN* | 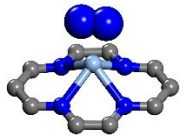 | -0.16 |
| NNH* | 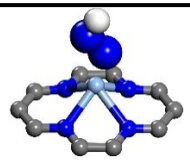 | 1.34 | NNH* | 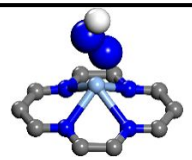 | 1.34 | NNH* | - | - |

| | | | | | | | | |
|---|---|---|---|---|---|---|---|---|
| NHNH* | 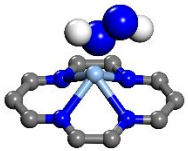 | 0.43 | $NNH_2$* | 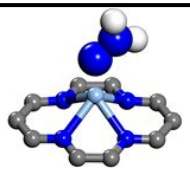 | 1.07 | NHNH* | - | - |
| $NHNH_2$* | 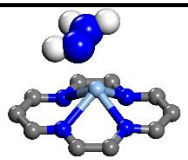 | 0.06 | N* | 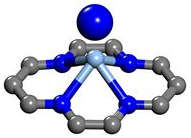 | 3.97 | $NHNH_2$* | - | - |
| $NH_2NH_2$* | 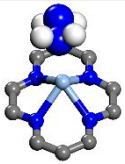 | -1.07 | NH* | 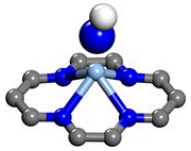 | 2.32 | $NH_2NH_2$* | - | - |
| $NH_2$* | 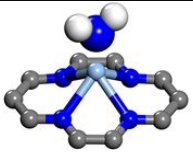 | -0.01 | $NH_2$* | 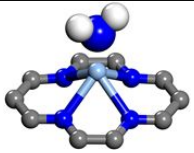 | -0.01 | $NH_2$* | - | - |
| $NH_3$* | 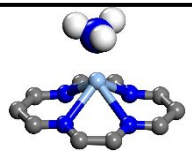 | -1.96 | $NH_3$* | 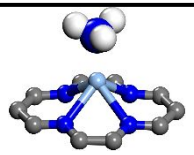 | -1.96 | $NH_3$* | - | - |